

Investigation of the charge transport through disordered organic molecular heterojunctions

H. Houili,¹ E. Tutiš,² I. Batistić,³ and L. Zuppiroli¹

¹*Laboratoire d'Optoélectronique des Matériaux Moléculaires, STI-IMX-LOMM, Station 3, Ecole Polytechnique Fédérale de Lausanne, CH-1015, Lausanne, Switzerland.*

²*Institute of Physics, Bijenička cesta 46, P.O. Box 304, HR-10000, Zagreb, Croatia.*

³*Department of Physics, Faculty of Science, Bijenička cesta 32, University of Zagreb, P.O. Box 331, HR-10002 Zagreb, Croatia.*

Abstract

We develop a new three-dimensional multiparticle Monte Carlo (*3DmpMC*) approach in order to study the hopping charge transport in disordered organic molecular media. The approach is applied here to study the charge transport across an energetically disordered organic molecular heterojunction, known to strongly influence the characteristics of the multilayer devices based on thin organic films. The role of energetic disorder and its spatial correlations, known to govern the transport in the bulk, are examined here for the bilayer homopolar system where the heterojunction represents the bottleneck for the transport. We study the effects of disorder on both sides of the heterojunction, the effects of the spatial correlation within each material and among the layers. Most importantly, the *3DmpMC* approach permits us to treat correctly the effects of the Coulomb interaction among carriers in the region where the charge accumulation in the device is particularly important and the Coulomb interaction most pronounced. The Coulomb interaction enhances the current by increasing the electric field at the heterojunction as well as by affecting the thermalization of the carriers in front of the barrier. Our MC simulations are supplemented by the master equation (ME) calculations in order to build a rather comprehensive picture of the hopping transport over the homopolar heterojunction.

PACS numbers: 73.61.Ph, 73.20.At, 72.20.Ee, 05.10.Ln

I. INTRODUCTION

The physical processes governing the devices based on thin organic amorphous films have been the subject of significant interest during the last decade.[1] This includes the charge transport, exciton creation, and electron-hole recombination in the strong electric field of the order of 1MV/cm. These and other processes form the basics of functioning of present and forthcoming organic electronic devices. In addition, these devices are usually composed of more than one organic material. This introduces the organic heterojunctions which often play the major role in the device characteristics. This shows both experimentally and in some elaborate device model simulations.[2, 3, 4, 5, 6, 7, 8] The structure of the heterojunction is known to affect the efficiency, electric characteristics of the device, and its durability. Therefore the understanding of the electronic processes at organic heterojunctions is essential for the proper understanding of the whole device. In spite of that the theoretical work aimed at understanding the organic heterojunctions, in terms of their structure, is scarce. This may be contrasted with numerous theoretical investigations on the effect of disorder and correlations on injection and charge mobility within the bulk.[9][10] This former research has established a general picture of electronic transport in disordered molecular materials and polymers. It proceeds via electron hopping among representative molecular states. In particular, one deals with the highest occupied molecular orbital (HOMO) and the lowest unoccupied molecular orbital (LUMO). The occupancy of HOMO and LUMO orbitals changes as the device is switched on. First, extra electrons and holes are being introduced from electrodes (injection) onto neighboring molecules. As the carriers spread further into the bulk they reach the heterojunctions. The most important characteristic of a heterojunction is the difference of LUMO and HOMO levels between different molecular species. This difference often shows as the energy barrier for the carriers (electrons entering the material with higher LUMO level or holes entering the material with lower HOMO). This almost regularly occurs in multilayer structures of organic light emitting diodes (OLED), where lower LUMO materials near the cathode (facilitating electron injection) meet the higher LUMO materials inside the device (more appropriate for light emission of the photon with several eV's in energy). Similarly, one encounters the energy barrier for holes at heterojunctions closer to an anode. This stepwise injection, with intermediate materials between the electrode and the electro-luminescent material, is known to facilitate the charge inflow into the device.

However, it also happens that in that way the bottleneck for charge transport moves from the electrodes towards the organic heterojunctions. The latter then dominate the electric characteristics of organic multilayer structures. It should be pointed out from the outset that the average value of the energetic barrier at the heterojunction is not its sole property to determine its permissivity to carrier flow. It is the energetic and structural disorder that also affect the performance of the heterojunction. Disorder is expected to modify the heterojunction characteristics, similarly as it predominantly determines the carrier mobility in an organic amorphous material. Another direct consequence of the barrier is the charge accumulation at the heterojunction, which is much more pronounced there than in the bulk. Therefore the *Coulomb effects* are also more pronounced at the heterojunctions than elsewhere. In that respect it is important to emphasize that in organic molecular materials the interacting electrons are well *localized* in space, with the localization length being of the size of a single molecule. Thus the nature of the Coulomb interaction is very much different from that in band semiconductors, where the spread of the electron wavefunction is considerably bigger than the mean carrier separation. The picture of interaction in disordered molecular media resembles the one between slowly moving "point charges". Therefore the interaction energy depends essentially on the charge configuration at a given instant of time and may not be properly expressed through the average occupancy of sites - the effect of correlations is pronounced.

For the reasons given above the most direct theoretical approach to an organic heterojunction is to develop a 3D numerical model for the hopping transport of many particles. In that respect it may be noted that numerical models for single-particle hopping were successfully used in the past to examine the effect of disorder on mobility and injection.[9, 11, 12, 13] These models have been conveniently implemented through the Monte Carlo (MC) algorithm. The MC approach has been used to simulate the hopping movement of a particle exploring the energy landscape of the molecular material. In order to consider the heterojunction problem many such particles have to be considered concurrently.

It should be noted immediately that the rather simple multiparticle MC approach proposed here is possible because in the systems under consideration the quantum phase of the electronic wave function is essentially lost in the (phonon-assisted) hop. Therefore, the orbital quantum effects are not expected to show in the assembly of particles. Instead, one may consider electrons as classical particles exhibiting hopping transport. On the other

hand, the spin state may be, and certainly *is*, in the absence of spin-orbit interaction centers, remembered in the hop.

There is one additional reason why the multiparticle MC approach is rather appropriate for studying organic molecular devices. The approach in which each particle is followed through the system profits from the fact that even for a large number of molecules (several million in our simulations) the number of particles is relatively low (several hundred). Indeed, in real systems like organic molecular diodes the density of particles is usually very low because of the lack of countercharges. Therefore the Coulomb forces limit the charge density. On the other hand, when both electrons and holes exist within a single organic layer, it is the recombination that limits the density. In both cases the molecules greatly outnumber the carriers. Only in the regions near bipolar heterojunctions, where both electrons and holes accumulate, the density of particles may be significantly increased. However, even then the MC approach may turn tractable.

As it will become apparent, the 3D multiparticle Monte Carlo (*3DmpMC*) approach may be applied to a wide set of problems aside from heterojunctions, e.g. to study the recombination crosssection, for considering the density and doping effects for the hopping transport, or for considering the influence of the discrete charge hopping on the space charge effects. As for heterojunctions, it may be applied both to a heterojunction where only one type of carriers is present (homopolar) as well as to those where electrons and holes meet and recombine (bipolar). Multiplying the effects of disorder, correlations, density effects, Coulomb interactions, recombination and interface structures brings us to great many number of possibilities, each within the reach of the method. However, we do not consider all these issues in the present paper. The paper introduces the *3DmpMC* method and discusses its application to the homopolar heterojunction problem. We consider the heterojunctions where only energetic disorder is present, postponing the discussion of the structural disorder for a separate paper. With all these limitations imposed it still turns out that the problem of a flat, energetically disordered, homopolar heterojunction presents a multitude of effects. We believe that all these have to be understood before addressing those related to the interface structured in the real space and before considering the bipolar problem.

Confining ourselves to the problem with a single type of carriers we bring in an additional simplification - we do not have to take care about spin degree of freedom. In the

simulation we do not permit a single molecule to be occupied by more than one carrier of a given type (no two extra electrons or two extra holes may reside on the same molecule simultaneously), whatever its spin projection. This constraint, imposed in accordance with the usual treatment of *localized* (donor, acceptor) states in doped semiconductors,[14] is maintained within the model even when we switch off the long-range tail (nearest neighbour and beyond) of the Coulomb interaction. Effectively, the constraint implies that single *state* is available per molecule for a given carrier. This implies that the spin degree of freedom will not show in the calculation for "electrons-only" or "holes-only" devices. It is understood that the "spinless-particle" approach may not be appropriate when electrons and holes are considered concurrently, with the recombination being dependent on the spin state of the particles.

From here the paper goes as follows. In the next three sections we introduce the Monte Carlo model and the numerical procedure as well as the master equation (ME) approach. We will discuss first the MC and ME results for the dependence of the particle current on disorder strength in variously parameterized heterojunctions. We then discuss in more detail the effect of long-range and short-range Coulomb interaction on the barrier crossing. The ratio of the forward and backward hopping rates is discussed in a separate section. This ratio also turns out to be important in the final section where we consider in more detail the effect of the precise form of the hopping law on the properties of the system.

II. THE MODEL

As the model of a heterojunction we consider the model of two cubic lattices placed side by side. For MC simulations we use two lattices of the size $200 \times 200 \times 50$ sites. Each of them represents a separate organic layer (denoted as layer I and layer II). The overall thickness of the model sample (100 molecular monolayers) is thus typical of real devices. The electrodes that are placed on both sides of the device impose the electric field and the carrier injection. For the two lateral directions, perpendicular to the applied electric field, we impose periodic boundary conditions to account for the extension of the device in those directions.

Here we describe a somewhat more general model than required for the calculations in the rest of the paper. In the present section we consider the system where both electrons and holes are present. Each site is then characterized by two energy levels, LUMO and HOMO.

The energetic disorder is introduced by adding the random values ϵ_i to the site LUMO and HOMO energies. These values follow the Gaussian distribution $(2\pi\sigma^2)^{-1/2} \exp(-\epsilon^2/\sigma^2)$. We consider both uncorrelated and correlated disorder. For the latter, the short-range correlations between the site energies are further imposed by taking the energy of the i -th site to be proportional to the average of the energies of all the sites contained within a sphere of radius a_{corr} , i.e. $\epsilon_i = N_{corr} \sum_k \epsilon_k$, where N_{corr} is a normalization factor.[13, 15] The correlation in the heterojunction region is handled separately. We consider both a) the case where the correlations inside each device layer are independent, and b) the case where the correlations extend over the organic/organic heterojunction. In the latter case we speak of "over-barrier" correlations. This case can occur especially when the energetic disorder is caused by random orientation of molecular dipoles. The correlations, occurring due to the long range of the dipolar potential, then extend beyond the interface between different materials.

The charge carriers (electrons and holes) interact through the Coulomb interaction, $q_i q_j / 4\pi\epsilon_0\epsilon_r r_{ij}$, screened by the dielectric constant of the material. Of course, the "self-interaction" of the electron is excluded. In particular this means that the energy levels of the two sites involved in hopping have no Coulomb contributions from the electron involved. On the other hand, these energy levels do experience the Coulomb shifts from all other particles in the device. In practice the calculation of the Coulomb shift is simplified by considering only the particles in the basic cell as point charges. For a given site this basic cell accounts for the portion of the device, with lateral extension 200×200 in our case, centered around the particular site. The Monte Carlo calculations for one-component plasma[16] showed that this approximation (termed "the minimum-image convention"), produces small differences with respect to the exact Ewald sum for a diluted plasma.

Due to weak binding forces in organic molecular semiconductors the carriers are localized on molecules. The hopping of electrons and holes from one localized site to another occurs when (as a result of the electron-lattice interaction) the atomic vibrations change the relative energy of these localized states. Three parameters determine the conditions of the charge transfer between the sites: the transfer integral J related to the wave function overlap between sites, the coupling strength g of the carrier to the lattice and the typical phonon energy $\hbar\omega_0$. [18, 19, 20] In the organic materials used as transport and emission layers in OLEDs, the transfer integral J is usually less than 0.1eV.[21] The phonon mode which

produces the relaxation is the C-C stretching mode which interchanges single and double bonds of the conjugated backbone ($\hbar\omega_0 = 0.15$ to 0.2eV). The coupling constant can be deduced from the relaxation energy of the molecule upon charging: $g = E_r/\hbar\omega_0$. Values of the relaxation energies have been calculated in Alq₃[22] and in PPV.[23] They range between 0.06 and 0.3 eV. A comprehensive review on the relative importance of the relevant parameters and the qualitative effects that we follow here, has been published by Emin.[24]

It may be recalled that the ratio $J/\hbar\omega_0$ is informative about the adiabaticity of the process. In the molecular materials considered here, where J is small, hopping is usually nonadiabatic: the intermolecular coupling energy is so small that the electronic carrier can only occasionally respond to favorable changes of atomic configurations by moving between sites. On the other hand, the coupling strength g in those materials is in the range from 0.5 to 2, implying a rather strong coupling. The hopping rate for such a process is given by[19]

$$\nu_{ij} = \frac{J^2}{\hbar} \sqrt{\frac{\pi}{2E_b kT}} \exp\left(-\frac{E_b + \epsilon_i - \epsilon_j}{2kT}\right) \exp\left[-\frac{(\epsilon_i - \epsilon_j)^2}{8E_b kT}\right], \quad (1)$$

where E_b is the polaron binding energy.

However, for historical reasons, hopping in molecular materials is usually considered through formula appropriate for a nonadiabatic process in the weak-coupling regime. The Miller-Abrahams formula, originally proposed for shallow impurity transport in semiconductors, gives the jump rate for such a phonon-assisted process,[25]

$$\nu_{ij} = \nu_0 \exp\left(-2\gamma a \frac{r_{ij}}{a}\right) \exp\left[-(\epsilon_i - \epsilon_j + |\epsilon_i - \epsilon_j|)/2kT\right], \quad (2)$$

where ν_0 is the attempt-to-jump frequency. Here only the rate upward in energy is activated.

Powered by the success of the Gaussian Disorder Model of Bässler and coworkers[11] and due to its simplicity, the Miller-Abrahams formula was used in almost all simulations related to transport in OLEDs[10, 26]. Nevertheless, in spite of their differences, the two formulae lead to some similar physical processes in a disordered system. Field-dependent mobility is also qualitatively similar for the two laws. On the other hand, one big difference is the appearance in Eq.(1) of the Marcus inverted region. In fact at higher fields, or more generally when $|\epsilon_i - \epsilon_j| \gg E_b$, the hopping rate starts decreasing due to the decreasing probability of phonon emission for a downward hop in energy.[19]

In order to provide the link with most of the papers on the hopping transport in the systems with Gaussian disorder, in this work we use mainly the hopping processes described

by Eq.(2). The question of the influence of different hopping laws on our conclusions is addressed in the separate section towards the end of the paper.

III. THE 3D MULTI PARTICLE MONTE CARLO ALGORITHM

The multiparticle Monte Carlo algorithm we use may be roughly described as follows. Basically, we follow the evolution of many particles, electrons and holes. As the system evolves through hops, at each step one has to select the particle that is to hop next. For that purpose we introduce the "dwelling time" t_{dwell}^i . It is an amount of time that the particle at site i spends there before the hop, $t_{\text{dwell}}^i = \left(\sum_j \nu_{ij}\right)^{-1}$. The particle with the smallest dwelling time is selected to perform the jump at a given instant of time. Once the particle at site k is chosen to perform the next hop, the destination of the hop is determined by a random number generator in accordance with the relative magnitudes of the ν_{kj} of sites inside a box of size $Nb \times Nb \times Nb$ (e.g. with $Nb = 6$). After the hop is performed the time variable t is advanced by the corresponding dwelling time - i.e. the time step in the simulation is defined by the dwelling time of the particle executing the hop.

More precisely, the algorithm goes as follows:

1. Let t denote the absolute time of the simulation and t_i the private time of particle at site i . The latter is set to zero when the particle arrives at the site and advances when the particle do not hop. Initially $t_i=0$ for all sites i populated by particles. The total number of occupied sites corresponds to N , the number of particles (electrons and holes) in the system.
2. Calculate the energy level shifts for the sites inside the hopping box ($Nb \times Nb \times Nb$) around each particle. Each energy level is determined by the external electric field and the Coulomb potential of the particles in the system.
3. Calculate the hopping probability for each site in the hopping box.
4. Deduce the dwelling time t_{dwell}^i for all occupied sites.
5. The site k , occupied by the particle to hop next, is determined by searching for the smallest $(t_{\text{dwell}}^i - t_i)$ among occupied sites.

6. Choose at random the site j within the hopping box of site k as the destination for the hop, obeying the relative probabilities calculated above. . The particle is de-assigned from site k and assigned to site j .

7. Update the times:
$$\begin{cases} t = t + (t_{\text{dwell}}^k - t_k) \\ t_j = 0 \\ t_i = t_i + (t_{\text{dwell}}^k - t_k), \text{ for occupied sites, } i \neq j \end{cases}$$

8. If $(t_{\text{dwell}}^k - t_k) < 0$ then the particle at site k hops to the site j chosen in the same manner, while the time variables are updated as follows:

$$\begin{cases} t_j = 0 \\ t, t_i \text{ unchanged, for occupied sites } i \neq j \end{cases}$$

The new configuration of particles is used to continue the simulation by re-entering the above algorithm from step 2.

The unit of time in the code is given by

$$t_0 = [6\nu_0 \exp(-2\gamma a)]^{-1} \quad (3)$$

The parameters ν_0 , and γ are the same throughout the system. In the simulations presented here $\nu_0 = 10^{13} \text{ s}^{-1}$ and $\gamma = 8.33 \text{ nm}^{-1}$.

As the model is currently set for the study of organic/organic interfaces, the details of the exact injection mechanism will not matter very much. However, it is important to establish the mechanism for the carrier inflow towards the interface. For example, one can use an appropriate injection formula with the parameters suitably chosen, e.g. the one discussed in Ref.[27]. The probability for the injection at the sites near the electrode is then determined by the electric field at the injecting electrodes. The latter is separately calculated within the code. Alternatively, one may fix the number of carriers (separately electrons and holes) in the device and create a carrier at a random position near the injecting electrode whenever a particle disappears either by leaving the device at the opposite electrode or in the recombination process. This approach of a fixed number of particles is chosen for the present paper, because in that case the total current in the system is the property of the heterojunction and not related to electrodes. However, to some extent, the results obtained within the two "injection approaches" may be transformed from one into another. For heterojunction investigations this basically reduces to calculating the current per particle,

instead of considering only the value of the current at a fixed number of particles. The calculation of the Coulomb effects on the injection field is simplified by the fact that most of the carriers are located in the heterojunction area.

The simulations related to the present paper begin with a random distribution of carriers. Snapshots of all the variables of interest are taken each 50 hops of the fastest carrier (i.e. in periods in which at least one of the carriers makes 50 hops). The steady state (the same average current along the whole device) is reached within the period of approximately 14 snapshots. After this stage the average of all the variables is taken in the time window of 50 snapshots. In this way we obtain satisfactory statistics for typical values of disorder and field strengths.

The algorithm described above has been implemented on a cluster of Linux-based machines. The numerical application of the *3DmpMC* method is much facilitated by the development of the computer cluster calculation techniques, where a handful of particles is taken care of by each computer node. The information required to calculate the Coulomb interaction between particles is communicated among nodes using Message Passing Interface (MPI) calls.

IV. THE MASTER EQUATION APPROACH

Many MC methods are known for their conceptual simplicity and a straightforward numerical approach. However, they are also known for the need to examine great many states of a system in order to reduce the statistical error. The present MC method shares this property. The other method that is sometimes used to examine the system of particles hopping in a disordered energy manifold is the master equation (ME) approach. The master equation approach has some advantages over the MC approach with respect to reducing the statistical uncertainties, as discussed in Ref.[28]

On the other hand, the ME approach fails to treat the Coulomb interaction correctly, both long-range and short range, although some attempts have been done to consider approximately the no-double-occupancy constraint within this approach.[28, 29] Here we use this approach where appropriate to supplement our results of the MC simulations. A more detailed account on the master equation approach may be found in Refs.[28, 30] where it was applied for studying the mobility and injection in a 3D disordered system, respectively.

Here we briefly outline the method and contrast it to the *3DmpMC* approach.

The basic assumption of ME approach is that the occupancy n_i of site i evolves in time according to the equation

$$\frac{dn_i}{dt} = \sum_{j:j \neq i} (-n_i \nu_{ij} + n_j \nu_{ji}) \quad (4)$$

where ν_{ij} 's are hopping rates already introduced within the MC approach. For an ensemble of non-interacting particles this is a perfectly rightful assumption if n_i represents the average occupancy of the site over a time scale much bigger than the inverse of the characteristic hopping frequency. Finding the steady state of the system ($dn_i/dt = 0$) then amounts to solving the (huge) linear system of equations for n_i 's, each of the equations being of the type as given above. The source part for the linear systems is provided by suitable additional terms that describe the coupling to the particle reservoir (electrodes). The solution simultaneously takes care of all possible hopping processes in the system. This is at odds with the MC approach which samples only a fraction of the bonds in the system, and those that are sampled are visited a finite number of times. However, as usual with the Monte Carlo, the statistics improves as the sampling extends.

As already mentioned, the effects of interaction are difficult to introduce correctly within the ME approach. For example, although some neighboring sites i and j may be occupied to the similar extent on average, $n_i \sim n_j$, in reality this may come from the same particle visiting both sites in turn. This means that at each moment one site is occupied while the other is empty and vice versa. Thus, calculating the interaction energy as the product $n_i \times n_j$ is obviously erroneous.

The simplest interaction that one wants to take account of is the strong repulsion among particles on meeting on the single molecule. If this interaction is strong enough the double occupancy of a molecule will be practically forbidden. Thus the particle at a site i will not be able to jump to a site j if the latter is occupied. In the quantum Hamiltonian language this is often described by effectively multiplying the hopping operator by $(1 - \hat{n}_j)$, \hat{n}_j being the particle density operator for site j . A similar extension to the master equation approach is obviously approximate since n_j in the master equation does not denote an operator but an average site occupancy.

However, on the qualitative level the extension of the ME equations to

$$\frac{dn_i}{dt} = \sum_{j,j \neq i} [-n_i \nu_{ij}(1 - n_j) + n_j \nu_{ji}(1 - n_i)] \quad (5)$$

seems advantageous. In the first place it assures that, irrespective of the number of carriers in the system (which should be less than the number of molecular sites, of course), the system will acquire a steady state with $n_i < 1$. For example, this prevents deep states (traps) to be overpopulated when the average number of carriers increases. Moreover, in the limiting case of no sources or sinks in the system, the equilibrium will be given by $n_i = \{1 + \exp[(E_i - \mu)/k_B T]\}^{-1}$, with μ set by the total number of particles. The latter result is what one expects for a site with no-double-occupancy constraint being in equilibrium with the reservoir represented by the rest of the system. For these reasons the preceding generalization of the ME seems suitable for considering a system with a finite concentration of particles. On the technical level, the extension is paid off by the fact that the steady-state equations become nonlinear. This requires devising a suitable mathematical procedure to solve the huge nonlinear system of equations for a given number of particles in the system. On the fundamental level, it must be kept in mind that the nonlinear ME approach is intrinsically approximate in the sense of the mean-field approximation, as explained above. Therefore, the multi-particle Monte Carlo approach, while possibly inferior (statistics-wise) for considering a system of non-interacting particles, seems to be an appropriate and superior approach for considering a system of real, interacting particles.

All applications of the ME approach in this paper are thus for particles that do not interact with long-range Coulomb forces. The linear and nonlinear ME solutions are compared to assess the importance of short-range repulsion for a given number of particles in the system. To reduce the complexity of the computational problem we consider only the nearest-neighbor hopping in all ME calculations. The results are generally consistent with MC simulations, given the strong decay of ν_{ij} 's with increasing distance among molecular sites. All ME calculations presented here are related to systems with correlated disorder in both layers, the correlation not extending over the heterojunction.

V. THE EFFECT OF DISORDER ON THE CURRENT THROUGH THE HETEROJUNCTION

The first important result of our MC simulations for homopolar heterojunctions are collected in Fig. 1. The figure shows the results for the current in the systems with correlated and uncorrelated disorder, with and without long-range Coulomb interactions, and contrasts the role of disorder in one vs. both layers in the bilayer device. For layers with correlated disorder the correlation length is fixed to three lattice constants.

We briefly comment on the main features discernible from Fig.1, deferring a more detailed discussion of each of them for separate sections. The figure shows the general dependence of the barrier permittivity on disorder strength. The only case where the current increases with increasing disorder strength is the one in which disorder is confined to the layer II while the layer I is kept ordered. The observed increase of the current with disorder is presumably due to the particular points where the barrier across the heterojunction is locally lowered. The current over the barrier is generally expected to depend exponentially (i.e. strongly nonlinearly) on the barrier height. Hence it is expected that the contribution of those crossing points to the average overcomes the effect of the points where the barrier is locally increased.

For all other cases the disorder strength is kept equal in both layers. In all these cases the current diminishes as the strength of disorder increases. Thus the effect of disorder in the layer I is to *reduce* the current. This effect always dominates the previously observed effect of disorder in the layer II. As discussed later in the paper and already observed in Ref. [26], the carriers accumulated in front of the barrier tend to thermalize to low energy states there, thus effectively increasing the barrier at the heterojunction. The figure also suggests that correlation within separate layers is not particularly beneficial for barrier crossing. On the other hand, the barrier crossing is facilitated when the correlation among layers is present. It may be further observed that switching on the long-range Coulomb interaction always increases the current in the system. This is chiefly because the Coulomb forces effectively lower the barrier. However, as will be shown soon, the size of this effect is much smaller than expected from the usual naive argument.

VI. THE EFFECT OF THE COULOMB INTERACTION ON THE BARRIER CROSSING

A. Long-range Coulomb forces

The effect of the interaction may be observed in our simulation as we increase the number of particles in the system. This is illustrated in Fig.2. The figure shows the current as the function of the number of particles in the system for particular values of the barrier height and disorder strength. The points related to the system of particles without long-range Coulomb interaction follows a straight line as the number of particles increases. The effect of the long-range Coulomb interaction is unobservable for small number of particles in the system. As expected, the effect starts to show as the number of particles increases.

It is also expected that long-range Coulomb interaction among electrons accumulated at the heterojunction will help the carriers to pass the barrier. This is expected since the electric field due to the interaction may lower the barrier in a way similar to how the external electric field F lowers the barrier by the amount Fqa . The usual straightforward estimate for the barrier lowering due to particle interaction goes as follows. Let us denote the average planar charge density at the heterojunction by $\rho_S = qN_s/a^2$, where N_s stands for the average number of carriers per cell cross section a^2 . If the charge at the heterojunction is assumed to be smeared homogeneously over the heterojunction plane, the extra electric field produced by this charge would be $F_{\text{hom}} = \rho_S/2(\epsilon_0\epsilon_r)$. Twice that much is the change of the electric field over the heterojunction. The naive estimate for barrier lowering is $F_{\text{hom}}qa$.

However, it must be recalled that the carrier wavefunction is not at all homogeneously smeared in the heterojunction plane. The carriers localized on molecular sites are spaced by $d \sim \sqrt{1/N_s}$ on average. It is the Coulomb repulsion among accumulated electrons that tends to order them in a regular mesh in the heterojunction plane. The continuum approximation F_{hom} for the electric field is valid only for distances $\delta x \gg d$ from the heterojunction. At shorter distances the effect of charge discreteness must be accounted for. Specifically, the distance to be considered for barrier lowering is $\delta x \sim a$. As the characteristic case for a homopolar heterojunction is $a \ll d$, the total change of the electric field at the heterojunction is expected to be smaller than the average field in the smeared charge picture. The effective electric field responsible for barrier lowering may be estimated e.g. by assuming that repelling

charges order approximately in the regular square lattice. The effective electric field then turns out to be very much smaller than F_{hom} , as showed in Fig. 3.

We illustrate these considerations with the case of 140 particles in our $100 \times 200 \times 200$ system. The particles accumulate in front of the heterojunction, as shown in Fig. 4. The planar particle density per unit cell cross section is $140/(200 \times 200) \approx 0.002$, with most of the particles concentrated in the last few monolayers of the layer I. The surface charge density is $\rho_S = 140q/(200a)^2$. In the continuum approximation the accumulated charge produces the extra field of approximately 0.25 MV/cm (taking $\epsilon_R = 3.5$). This field is already quite strong. Twice as many particles would double the electric field in layer II with respect to the imposed 0.5 MV/cm and reduce the electric field in the layer I to zero. For that reason the number of particles in the system may hardly go much above this concentration. Further particles would cause a negligibly small or even negative electric field at the injecting electrode. Taking the calculated extra field of 0.25 MV/cm as responsible for barrier lowering would imply a barrier shift of 0.015 eV. This would imply a current amplification of approximately $(\exp(0.015\text{eV}/k_B T) \approx 1.8)$ 80 percent. However this is not what one observes in the MC simulation where the amplification of a few percent is observed.

On the other hand, taking into account the discrete nature of the charge distribution in the heterojunction plane gives a much smaller electric field. It turns to be approximately 20 times smaller than the one obtained for the homogeneously charged plane. The barrier reduction due to particle interaction is much smaller than obtained above, as well as the current amplification which is then estimated to $(\exp[(0.015\text{eV}/20)/k_B T] \approx 1.03)$ a few percent, as observed in the simulation.

In summary, the Coulomb effect usually calculated for a homopolar heterojunction is strongly overestimated. This is true for most multilayer device models, as well as for some recent analyses of the dominant device physics.[31] On the other hand, the effect of discreteness that reduces the Coulomb effects in homopolar heterojunctions is expected to strongly amplify the Coulomb effects among electrons and holes at bipolar junctions.

B. The hard-ball repulsion

The short-range repulsion is always present in our *3DmpMC* model. Therefore its effect can not be deduced directly from the results on the current density. On the other hand, we

did the calculation with and without no-double-occupancy term within the ME approach. We found that the current enhancement due to short-range repulsion at a given particle density is less than one percent for the parameters given in Fig.1.

The effects of the short-range repulsion can be assessed even within the MC approach by considering the distribution in energy of the particles accumulated in front of the energy barrier. The particles in the sample spend much more time in front of the barrier than elsewhere. The number of hops per unit time among sites within that monolayer greatly outnumbers those that go down-field. This makes it possible for particles to explore the sites in front of the barrier rather well and establish a local quasi-equilibrium.

The properties of the quasi-equilibrium with and without the hard-ball repulsion may be approximately calculated in a simplified manner, and the results may be compared against the MC results. The calculation goes as follows. For non-interacting (*ni*) particles, the probability of a site being occupied is given by the Boltzmann expression $f_B(E) = \exp(-E/k_B T + \mu_{ni}/k_B T)$, where μ_{ni} stands for the local chemical potential, which depends on local concentration of particles. The distribution of the sites in energy, around zero average energy, being given by $P_0(E) = (2\pi\sigma)^{-1/2} \exp(-E^2/2\sigma^2)$, the probability distribution for the energy E representing an occupied site goes as

$$O_{ni}(E) = P_0(E)f_B(E) = \frac{1}{\sqrt{2\pi\sigma^2}} \exp \left[-\frac{(E + \sigma^2/k_B T)^2}{2\sigma^2} + \frac{\mu_{ni}}{k_B T} + \frac{\sigma^2}{2k_B^2 T^2} \right] \quad (6)$$

Thus the mean energy of the occupied state is shifted by $-\sigma^2/k_B T$ with respect to the case without disorder. This well-known shift of the energy of occupied states due to thermalization[11] tends to increase the effective barrier at the heterojunction.

This shift *decreases* to some extent once the hard-ball (*hb*) repulsion is taken into account. The no-double-occupancy constraint changes the probability of the state of energy E being occupied to $f_{hb}(E) = \{1 + \exp[(E - \mu_{hb})/k_B T]\}^{-1}$, i.e. to the Fermi-Dirac distribution function.[32]. The chemical potential and mean energy have to be calculated numerically for this probability distribution. The result for two cases (i.e. with and without hard-ball repulsion) is illustrated in Fig. 5. In general, the hard-ball repulsion *reduces* the shift of the mean particle energy due to disorder. The interaction also shifts the chemical potential upwards. The MC results are also shown in Fig. 5. The thermalisation obtained within MC simulations is somewhat weaker than the one predicted by simple hard-ball statistics calculation. We believe that this discrepancy may be due to the confining effect of the electric

field. By pushing the carriers towards the interface, the field prevents them from exploring a larger energy manifold with lower energy levels. By switching on and off the long-range Coulomb interaction we checked that those contribute negligibly to thermalisation at a given particle density.

Fig. 5 also shows that for a particular particle density and for room temperature, the difference between the thermalization shifts is very small for disorder strengths less than 0.06 eV. The difference becomes pronounced in systems with stronger disorder or at higher particle density at the heterojunction. Since the value for σ in some disordered organic molecular material may be rather big (e.g. $\sigma \sim 0.15$ eV for Alq₃), [33], the effect of short-range repulsion is realistic to expect for some heterojunctions. On the other hand, the particle density at homopolar heterojunctions may be much higher only if the operational field is raised much above 0.5 MV/cm. This is because, the operational field limits the particle surface density at the heterojunction, as already pointed above.

VII. BACKWARD AND FORWARD HOPPING RATES

Recently Arkhipov et al. got interested in the ratio of backward (b) to forward (f) hopping rates at the heterojunction[26]. Their physical motivation was to resume the hops that lead to injection at a heterojunction ($\propto b - f$) from those that may lead to immediate recombination with a carrier of the opposite polarity. While their argument may certainly need to be amended by considering the Coulomb interaction among carriers of opposite polarity in the latter case, the b/f ratio is indeed important when considering the permittivity of the barrier to current flow.

Other motivation to consider the b/f ratio comes from reflecting on the aging processes in organic devices. A decade ago it was shown by Tang and Van Slyke that the aging rate of OLED's is proportional to the operating current.[3] This rule, also termed the "Coulomb aging" rule, may suggest that the hopping rate at the microscopic scale is directly related to degradation[34]. However, while the average current density is constant throughout the device, it is not necessarily so for the hopping rate. This is because at any given point in the device both forward and backward hops contribute to the local hopping rate ($\propto f + b$), while the current, being constant along the device, is proportional to their difference ($\propto f - b$). The hopping activity, here defined as $(f + b)/(f - b) = (1 + b/f)/(1 - b/f)$ is therefore

expected to be dependent on position in an inhomogeneous device, and especially when considering the region near the heterojunction. Fig.6 shows this dependence as obtained in our ME calculation. It may be observed that the hopping activity is many times bigger near the heterojunction than elsewhere. However, it is not the very heterojunction where the hopping activity is maximal. The hopping activity maximizes in the last few monolayers of the layer I, just before the barrier. This is mostly due to the increased concentration of particles in that region and the relatively low probability for further down-field hops.

Concentrating on the hops over the heterojunction, which determine the heterojunction permittivity to particle flow, we investigated the effect of the structure of the heterojunction and the Coulomb interaction on the b/f ratio. The result is shown in Fig. 7. While generally the b/f ratio increases with the increasing strength of disorder, one may also notice the effect of correlations and the Coulomb interaction. First, correlation generally lowers the b/f ratio, especially as disorder increases. The effect is possibly related to the fact that the carriers that enter the layer II face a locally more ordered environment, which implies smaller probability for returning hops. Second, the Coulomb interaction increases the relative importance of backward jumps to some extent, especially at low disorder strength. We do not have a simple explanation for the latter effect. Considering the forward hopping rate separately in Fig. 8, we find that it increases on switching on the Coulomb interaction, to the effect of increasing the current, in spite of an increased b/f ratio, $J \propto f \times (1 - b/f)$. However, the increase of the b/f ratio cannot be explained simply in terms of increased effective electric field at the interface. This will become clear shortly as we consider the dependence of b/f ratio on the electric field.

For the nearest-neighbor hopping and without long-range Coulomb interaction, an analytic expression for the b/f ratio can be derived in the limit of zero disorder. The derivation starts from the fact that the density in an ordered system is constant throughout layer II. This establishes the relation between the current and the particle density in the same layer. The current may be also expressed by the difference between forward and backward hopping rates at the very heterojunction. Then, assuming $\Delta > Fqa$, the result for the M.-A. hopping formula follows,

$$(b/f)_{\text{HJ}} = 1/[2 - \exp(-Fqa/k_B T)] \quad (7)$$

The zero-disorder value of b/f is 0.59 for the parameters of Fig. 7, in accordance with MC results.

As for the dependence on disorder strength σ , the MC results are supplemented here by the ME results for b/f away from the heterojunction (Fig.9). The dependence on the electric field given in Fig.10, while roughly following the analytical result for $\sigma = 0$, changes differently with disorder for low and high electric field, the crossover being roughly defined by $Fqa \sim \Delta/3$.

VIII. THE EFFECT OF THE HOPPING LAW ON THE BARRIER CROSSING

One of the questions that arise when discussing the effects in a system with hopping conduction is the qualitative dependence of these effects on the precise form of the hopping law. While the results presented above were obtained by assuming the Miller-Abrahams hopping law, qualitatively similar results are obtained if one uses the symmetric hopping law or the small-polaron hopping formula. This is illustrated in Fig.11 (ME calculations). The figure shows the current through the heterojunction as a function of the barrier height Δ , at a given disorder strength. The hopping laws used for this calculation are

$$\nu_{ij}^{MA} = \nu_{nn} \exp \left(-\frac{E_i - E_j + |E_i - E_j|}{k_B T} \right), \quad (8)$$

$$\nu_{ij}^{SYM} = \nu_{nn} \exp \left(-\frac{E_i - E_j}{2k_B T} \right), \quad (9)$$

$$\nu_{ij}^{POL} = \nu_{nn} \exp \left[-\frac{E_i - E_j}{2k_B T} - \frac{(E_i - E_j)^2}{8k_B T E_b} \right]. \quad (10)$$

To simplify the comparison, the bare value for the nearest-neighbor hopping frequency ν_{nn} was chosen the same for all three hopping laws, while the hopping was confined to the nearest neighbors. The number of carriers in the system was also kept the same.

For $\Delta = 0$ the current through the system reflects the value of the mobility in a homogeneous system for different hopping laws. The issue of mobility vs. hopping law in a disordered system has been addressed in the literature.[35] It was shown numerically that the Miller-Abrahams and the symmetric formula give qualitatively the same field dependence of mobility, as far as the disorder strength is bigger than the potential drop among neighboring molecules due to the electric field, $\sigma > Fqa$. While sharing the common field dependence, the value for mobility $\mu_{MA}(F)$ in that region is found generally smaller than $\mu_{SYM}(F)$. We are not aware of any similar considerations for heterojunctions, either numerical or analytical. Fig. 11 shows the dependence of the current through the junction on the

barrier height. It shows that the dependence is similar for all three hopping laws. Although the polaron binding term reduces the current somewhat as the barrier height increases, the dependences shown by all three curves are qualitatively similar.

What may seem particularly strange is the fact that the ratio of J_{SYM}/J_{MA} changes very little over the range where the factor $\exp(\Delta/2k_B T)$, relating different hopping laws at the heterojunction, changes over three and a half orders of magnitude. This may be even stranger when the distributions of the carriers in space are examined for the three hopping laws. No significant differences can be observed - almost all the carriers are grouped in the first few monolayers in front of the barrier, as illustrated in Fig.4. Therefore the forward hopping rate at the heterojunction is approximately $\exp[(\Delta - Fqa)/2k_B T]$ times bigger for the symmetric hopping law than for the Miller-Abrahams (MA) hopping law. Hence the backward hopping rate in the symmetric case has to compensate the forward hopping rate rather precisely in order to bring the current to the same order of magnitude as for the MA case.

Fortunately, these considerations may be supported by exact analytic expressions for a limiting case of the heterojunction between two ordered layers. As already pointed out in the previous section, in that case the ratio of backward to forward hopping rates may be derived analytically.[36] For the Miller-Abrahams hopping rate the result was given already in Eq.7 whereas for the symmetric law it is

$$\left(\frac{b}{f}\right)_{HJ,SYM} = \frac{1}{1 - e^{-\Delta/2k_B T} (e^{Fqa/k_B T} - 1)}, \quad (11)$$

Neglecting the minor differences between carrier distributions, the ratio of currents in the two cases becomes

$$\frac{J_{SYM}}{J_{MA}} \approx e^{(\Delta - Fqa)/2k_B T} \frac{1 - (b/f)_{HJ,SYM}}{1 - (b/f)_{HJ,MA}}. \quad (12)$$

The analytical expressions for b/f 's can be substituted into this equation. It is then readily verified that the big difference in forward hop frequencies between the two cases is compensated by respective backward hop rates. This analytic expression for J_{SYM}/J_{MA} also reproduces approximately the value obtained numerically (Fig.11) for finite disorder. We believe that this qualitative result also stands in the core of the aforementioned similarity between mobilities for the two hopping laws in homogeneously disordered systems. In the latter case the bottlenecks for transport are again barriers bigger than Fqa , statistically generated and scattered in space. The argument relating the two hopping laws is still expected

to apply on those barriers.

IX. CONCLUSION

In summary, we presented a new multiparticle Monte Carlo method that is suitable for addressing a number of presently unexplored questions related to electronic transport in organic disordered materials. In this publication we applied the method to a homopolar heterojunction, considering the influence of disorder and Coulomb interaction on the current through the heterojunction. Supplementing our MC results with the master-equation (ME) calculations, we developed a rather detailed insight into the effects of short-range and long-range Coulomb repulsion, forward vs. backward hopping processes and the precise form of the hopping law. In particular, we showed the estimates based on a continuum approximation strongly overestimate the effect of the long-range Coulomb interactions on the current through the heterojunction. Also, the long-range Coulomb interactions do not affect visibly the thermalisation of carriers in front of the barrier. It is rather the no-double-occupancy constraint which dominantly determines the effective barrier height. The presence of disorder and especially the energy barrier at the heterojunction lead to position-dependent forward and backward hopping rates. The frequency of charging and discharging of molecules then varies throughout the device. This likely affects the aging and the degradation. As in the case of bulk transport, the microscopic hopping law appeared to play a minor role in heterojunction barrier crossing provided that the polaron binding energy is smaller than the energy barrier. This study presents basis for further theoretical studies of more complicated (mixed, graded, rough) homopolar heterojunctions that are being developed experimentally. The multiparticle MC method introduced in this paper is currently applied for studying the recombination processes at bipolar heterojunctions.

Acknowledgments

We thank Dr. D. Berner for many helpful discussions. We are also grateful to Dr. B. Horvatić for discussions and remarks on the manuscript which significantly improved the paper. The MC calculations in this paper were done on "Janus", an HP SC45 cluster at DIT-EPFL. The ME calculations were performed on the "Grozd" Opteron cluster at the

- [1] S. R. Forrest, *Nature* **428**, 911 (2004); D. Berner, H. Houili, W. Leo, and L. Zuppiroli, *Phys. Stat. Sol. A* **202**, 9 (2005).
- [2] C. W. Tang and S. A. Van Slyke, *Appl. Phys. Lett.* **51**, 913 (1987).
- [3] S. A. Van Slyke, C. H. Chen, and C. W. Tang, *Appl. Phys. Lett.* **69**, 2160 (1996).
- [4] G. Vamvounis, H. Aziz, N.-X. Hu, and Z. D. Popovic, *Synth. Met.* **143**, 69 (2004).
- [5] E. Tutiš, D. Berner, and L. Zuppiroli, *J. Appl. Phys.* **93**, 4594 (2003).
- [6] J. Staudigel, M. Stossel, F. Steuber, and J. Simmerer, *J. Appl. Phys.* **86**, 3895 (1999).
- [7] E. Tutiš, M. N. Bussac, B. Masenelli, M. Carrard, and L. Zuppiroli, *J. Appl. Phys.* **89**, 430 (2001).
- [8] H. Houili, E. Tutiš, H. Lütjens, M. N. Bussac, and L. Zuppiroli, *Comp. Phys. Comm.* **156**, 108 (2003).
- [9] Y. N. Gartstein, and E. M. Conwell, *Chem. Phys. Lett.* **255**, 93 (1996).
- [10] U. Wolf, V. I. Arkhipov, and H. Bässler, *Phys. Rev. B* **59**, 7507 (1999).
- [11] H. Bässler, *Phys. Stat. Sol. B* **175**, 15 (1993).
- [12] E. M. Conwell and M. W. Wu, *Appl. Phys. Lett.* **70**, 1867 (1997).
- [13] Y. N. Gartstein and E. M. Conwell, *Chem. Phys. Lett.* **245**, 351 (1995).
- [14] B. Sapoval, and C. Hermann, *Physics of Semiconductors* (Springer, New York, 1995).
- [15] S. V. Rakhmanova, and E. M. Conwell, *Appl. Phys. Lett.* **76**, 3822 (2000).
- [16] S. G. Brush, H. L. Sahlin, and E. Teller, *J. Chem. Phys.* **45**, 2102 (1966).
- [17] Y. N. Garstein, E. M. Conwell, and M. J. Rice, *Chem. Phys. Lett.* **249**, 451 (1996).
- [18] D. Emin, *Phys. Rev. B* **46**, 9419 (1992); **48**, 1840 (1993).
- [19] D. Emin, *Adv. Phys.* **24**, 305 (1975).
- [20] L. Zuppiroli, M. N. Bussac, S. Paschen, O. Chauvet, and L. Forro, *Phys. Rev. B* **50**, 5196 (1994).
- [21] A. Ferretti, A. Ruini, G. Bussi, E. Molinari, and M.J. Caldas, *Phys. Rev. B* **69**, 205205 (2004).
- [22] A. Curioni, M. Boero, and W. Andreoni, *Chem. Phys. Lett.* **294**, 263 (1998).
- [23] L. Zuppiroli, A. Bieber, D. Michoud, G. Galli, F. Gygi, M. N. Bussac, and J. J. André, *Chem. Phys. Lett.* **374**, 7 (2003).

- [24] D. Emin, in Handbook of Conducting Polymers, edited by T. A. Skolheim (Dekker, New York, 1986), vol.2, p.915.
- [25] A. Miller, and E. Abrahams, Phys. Rev. **120**, 745 (1960).
- [26] V. I. Arkhipov, E. V. Emelianova, and H. Bässler, J. Appl. Phys. **90**, 2352 (2001).
- [27] J. C. Scott and G. G Malliaras, Chem. Phys. Lett. **299**, 115 (1999).
- [28] Z. G. Yu, D. L. Smith, A. Saxena, R. L. Martin, and A. R. Bishop, Phys. Rev. Lett. **84**, 721 (2000); Phys. Rev. B **63**, 085202 (2001).
- [29] W. F. Pasveer, J. Cottaar, C. Tanase, R. Coehoorn, P. A. Bobbert, P. W. M. Blom, D. M. de Leeuw, and M. A. J. Michels, Phys. Rev. Lett. **94**, 206601 (2005).
- [30] E. Tutiš, I. Batistić, and D. Berner, Phys. Rev. B **70**, 161202 (2004).
- [31] T. van Woudenberg, J. Wildeman, and P. W. M. Blom, Phys. Rev. B **71**, 205216 (2005).
- [32] The Fermi-Dirac distribution for the hard-ball problem is the consequence of considering spinless particles. Each site then contributes to the density of states with a single state. Considering the particles with spin one-half one would have two (2) states per site (one per spin projection). In that case the probability for the site being occupied would read as $1/\{1 + \frac{1}{2} \exp[(E - \mu_2)/k_B T]\}$, where 2 comes from the number of spin projections. It may be easily checked that for a given concentration of particles the two approaches (with and without spin) to the hard-ball interaction give the same distribution. The factor $\frac{1}{2}$ in the second approach is compensated by the difference in the chemical potential with respect to the spinless approach.
- [33] G. G. Malliaras, Y. Shen, D. H. Dunlap, H. Murata, and Z. Kafafi, Appl. Phys. Lett. **79**, 2582 (2001).
- [34] D. Berner, private communication.
- [35] S. V. Novikov, D. H. Dunlap, V. M. Kenkre, P. E. Parris, and A. V. Vannikov, Phys. Rev. Lett. **81**, 4472 (1998).
- [36] The expression for $(b/f)_{HJ,MA}$ as given in the text is independent of Δ . On the other hand the limit $\Delta \rightarrow 0$ represents the homogenous system without barrier. In that limit the b/f ratio at the heterojunction must reproduce the value in the ordered bulk, $(b/f)_{bulk} = \exp(-Fqa/k_B T)$. This is indeed what happens and the equation in the text has to be supplemented by the equation valid for $\Delta < Fqa$. One then obtains $(b/f)_{HJ,MA} = [1 + e^{(Fqa - \Delta)/k_B T} (1 - e^{-Fqa/k_B T})]^{-1}$. This equation is derived in the same manner as the

one for $\Delta > Fqa$.

- [37] O. Schenk, and K. Gaertner, Journal of Future Generation Computer Systems, **20**(3), pp. 475-487, 2004; O. Schenk, K. Gaertner, and W. Fichtner, BIT 2000, Vol. 40, No. 1, pp. 158-176; SIAM Journal on Scientific Computing, **1**(20), 359-392, 1998.

Figure captions

Figure 1: (MC) Current across the heterojunction as a function of disorder strength. Following cases are considered: *no corl+Coulomb*: non correlated disorder and (long-range) Coulomb interactions included; *corl+Coulomb*: correlated disorder within each layer and Coulomb interactions included; *corl-Coulomb*: correlated disorder within each layer and without long-range Coulomb interaction; *one-side corl+Coulomb*: correlated disorder in the second layer while the first layer is ordered, the Coulomb interactions are included; *over-barrier correlated +Coulomb*: the correlations in the energy disorder present in both layers extending over the heterojunction, long-range Coulomb forces being included in the calculation. The number of particles in the system ($100 \times 200 \times 200$ sites) is always 140. The bare barrier height (the difference among average LUMO/HOMO energy of two materials) at the heterojunction is 0.15 eV. The strength of externally applied electric field is 0.5 MV/cm.

Figure 2: (MC) The dependence of the current in the system on the number of particles in the system ($100 \times 200 \times 200$ sites). The squares stands for the results where the interaction among particles is full Coulomb interaction. The lower curve (filled circles) stands the current in the system where only "hard-ball" short-range interaction is taken into account (i.e. double occupancy of a site is forbidden but no long-range repulsion is accounted for). The imposed electric field is 0.5 MV/cm. The bare barrier height is $\Delta = 0.15$ eV.

Figure 3: The effective field at the homopolar heterojunctions leading to barrier lowering, as produced by the accumulated charges, vs. the electric field of the equivalent homogenously smeared planar charge. F_{eff} is estimated here by assuming that electrons at the heterojunction are ordered as point charges forming a regular square mesh.

Figure 4: (MC) The average occupancy of the molecular site in the system as a function of the position of the site with respect to the plane of the heterojunction (the first monolayer of the layer II is positioned at zero). The density in front of the barrier is much bigger than in the bulk of both layers. From the heterojunction to the left the occupancy falls approximately exponentially. The model parameters are: $\sigma = 0.04\text{eV}$,

$\Delta = 0.15\text{eV}$, $a = 0.6\text{nm}$, $F = 0.5\text{MV/cm}$. The data represent the results for 140 particles in the system of $100 \times 200 \times 200$ sites.

Figure 5: The energy shift due to thermalisation in front of the barrier, shown as the function of disorder strength. *Boltz. shift* is for non-interacting particles when the Boltzman law gives the orbital occupancy. *HB shift* is the calculation for the particles with hard-ball interaction in the equilibrium for the average molecular occupancy of 2×10^{-3} . The filled circles is what we get from the MC simulations.

Figure 6: (ME) The hopping activity in the system is shown as the function of the position along the system. Here f and b stand for the forward and backward hopping frequency between successive monolayers, respectively. $f + b$ is the average frequency of hops in both direction, while $f - b$ is constant throughout the system, being proportional to the particle current in the field direction. Three graphs correspond to three hopping rules (MA: Miller-Abrahams, SYM: symmetric hopping law, POL: small polaron hopping formula with polaron binding energy $E_b = 0.05\text{ eV}$). $\sigma = 0.05\text{ eV}$, $a = 0.6\text{ nm}$, $\Delta = 0.15\text{ eV}$. Backward hops at the heterojunction are the most pronounced for the symmetric hopping law, while less pronounced for the Miller-Abrahams and small-polaron hopping formulae.

Figure 7: (MC) Variation of the ratio of backward to forward hopping rates with disorder. $F = 0.5\text{ V/cm}$. $\Delta = 0.15\text{ eV}$. The number of particles in the system is 140.

Figure 8: (MC) Number of forward hops as a function of disorder. The forward hopping rate is strongly increased by long-range Coulomb forces, especially at low disorder. It is also increased by the disorder correlations between layers ("*over barrier corl*").

Figure 9: (ME) The ratio of the backward to forward hop frequency as the function of the strength of disorder. Different graphs refer to different positions with respect to the barrier, as indicated by the labels (e.g. -3 denotes the position that is three monolayers before the barrier). The spatial dependence of b/f is not at all pronounced in layer II. Throughout the layer II the $b(\sigma)/f(\sigma)$ curve resembles the one labeled by -8, corresponding to the monolayer of layer I that is rather far from the heterojunction.

Figure 10: (ME) The ratio of backward and forward hopping frequency at the very barrier as a function of the electric field at the barrier. The dashed line represents the result without disorder, described by the formula in the text.

Figure 11: (ME) The dependence of the current through the junction as the function of the barrier height. The three curves represent the results for three different hopping laws. The density of particles per device cross section, $140/(200*0.6\text{nm})^2 \approx 0.01\text{nm}^{-2}$, is the same in all three cases.

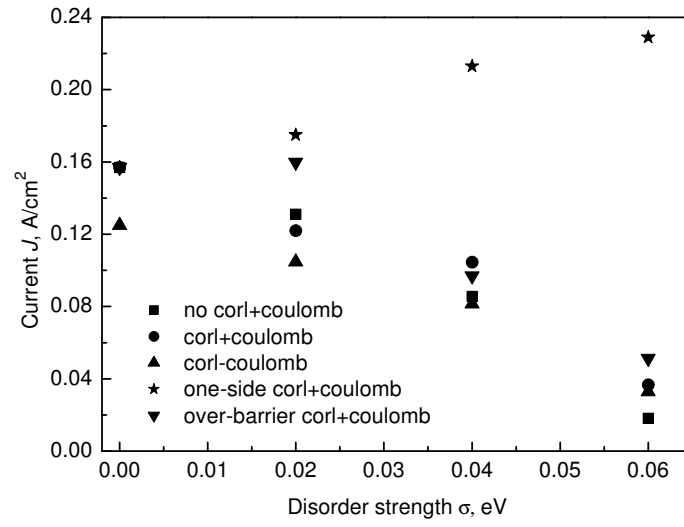


FIG. 1:

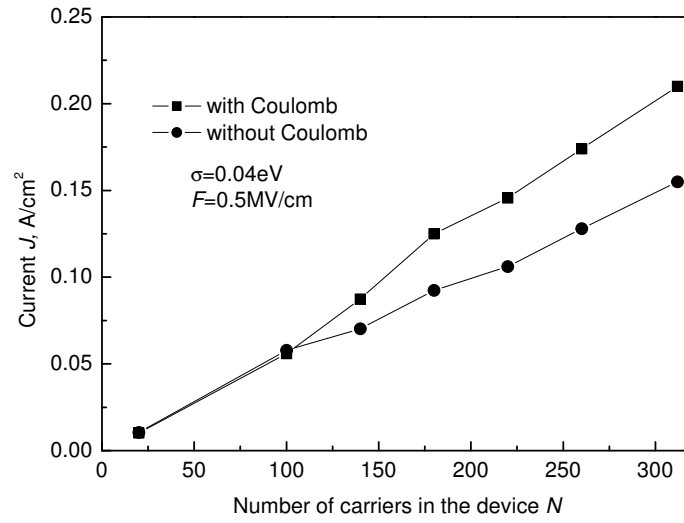


FIG. 2:

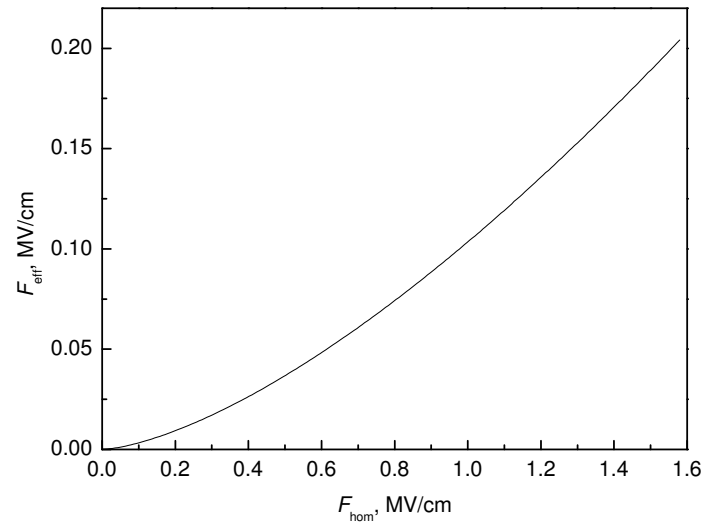


FIG. 3:

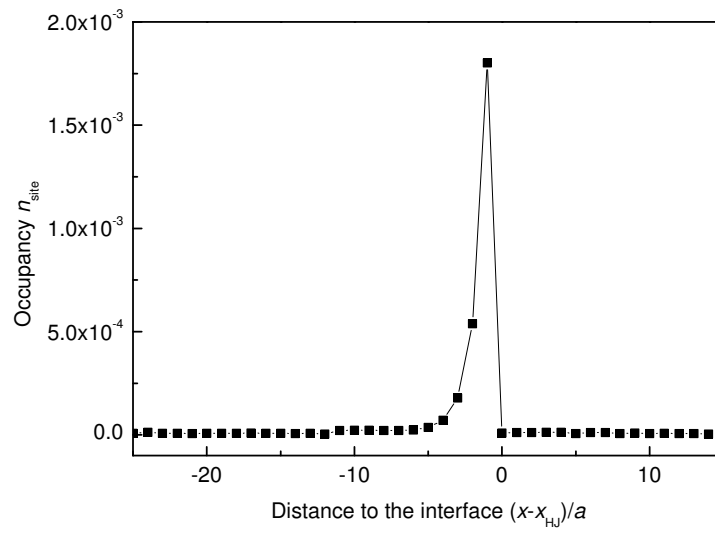


FIG. 4:

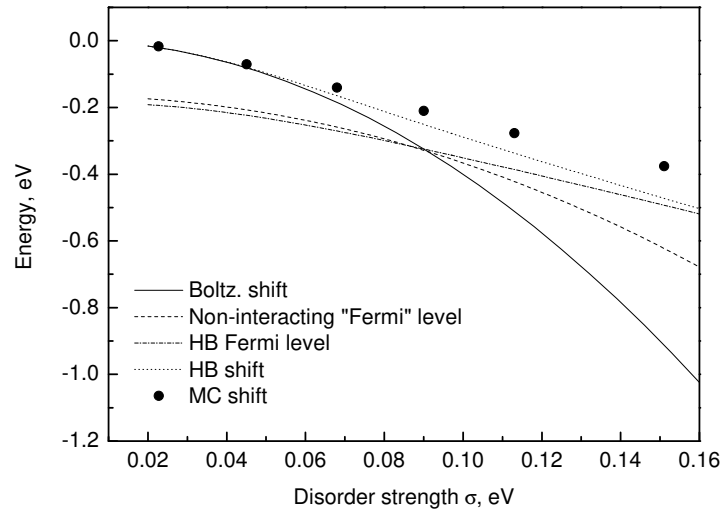


FIG. 5:

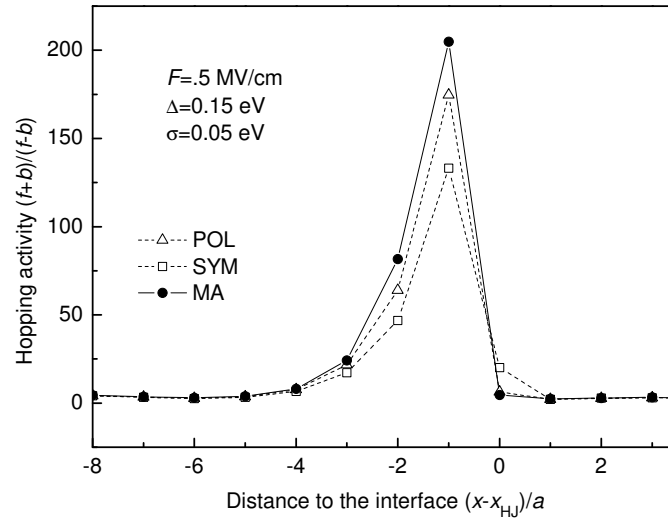


FIG. 6:

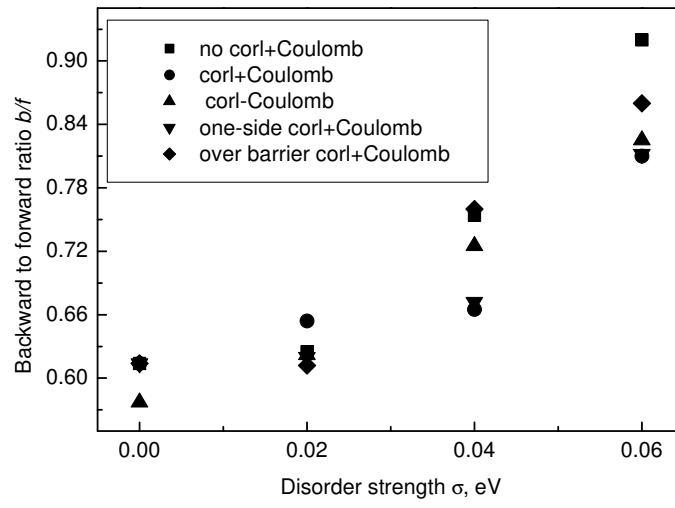


FIG. 7:

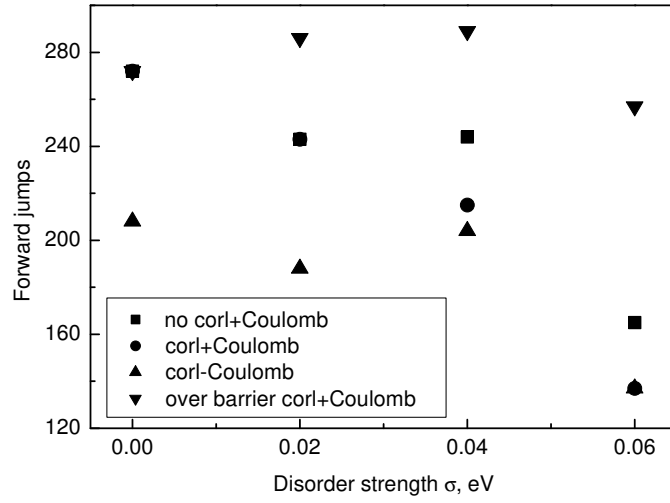


FIG. 8:

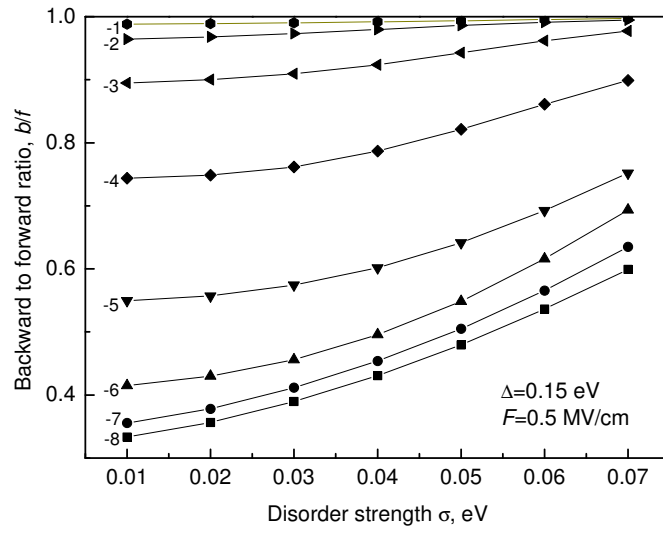


FIG. 9:

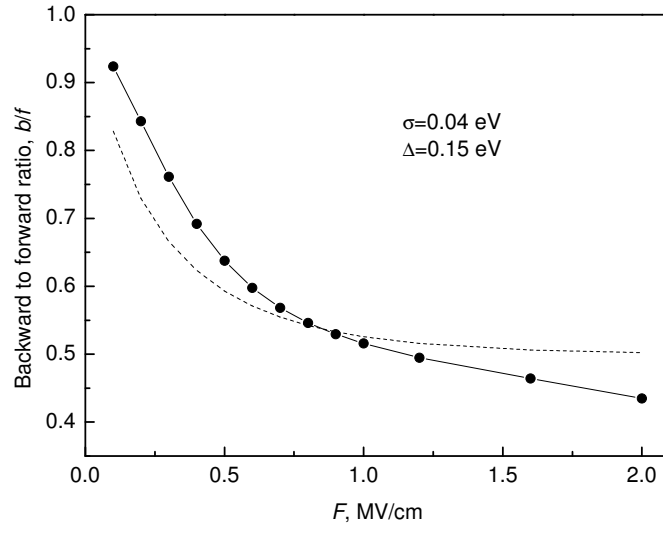


FIG. 10:

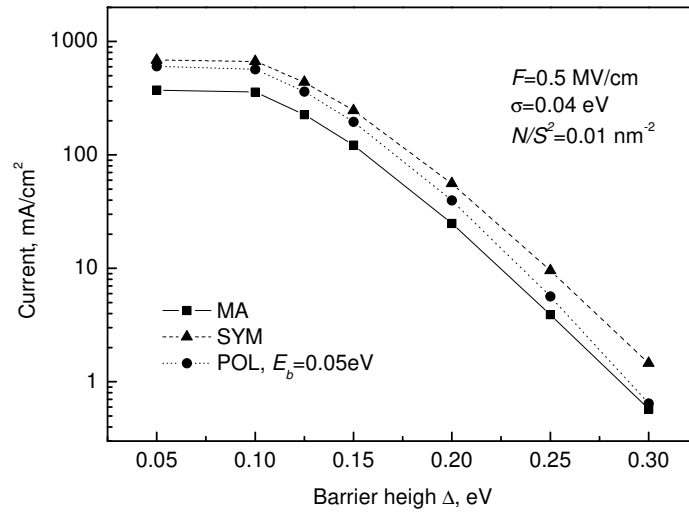


FIG. 11: